Azimuthal decomposition with digital holograms

Igor A. Litvin,[1] Angela Dudley,[1,2] Filippus S. Roux,[1] and Andrew Forbes[1,2,*]

[1]*CSIR National Laser Centre, PO Box 395, Pretoria 0001, South Africa*
[2]*School of Physics, University of KwaZulu-Natal, Private Bag X54001, Durban 4000, South Africa*
**aforbes1@csir.co.za*

Abstract: We demonstrate a simple approach, using digital holograms, to perform a complete azimuthal decomposition of an optical field. Importantly, we use a set of basis functions that are not scale dependent so that unlike other methods, no knowledge of the initial field is required for the decomposition. We illustrate the power of the method by decomposing two examples: superpositions of Bessel beams and Hermite-Gaussian beams (off-axis vortex). From the measured decomposition we show reconstruction of the amplitude, phase and orbital angular momentum density of the field with a high degree of accuracy.

©2012 Optical Society of America

OCIS codes: (070.6120) Spatial light modulators; (120.3940) Metrology; (090.1995) Digital holography; (120.5060) Phase modulation.

References and links

1. J. W. Goodman, *Introduction to Fourier Optics* (McGraw-Hill Publishing Company, 1968).
2. E. Tervonen, J. Turunen, and A. Friberg, "Transverse laser mode structure determination from spatial coherence measurements: experimental results," Appl. Phys. B **49**(5), 409–414 (1989).
3. A. Cutolo, T. Isernia, I. Izzo, R. Pierri, and L. Zeni, "Transverse mode analysis of a laser beam by near- and far-field intensity measurements," Appl. Opt. **34**(34), 7974–7978 (1995).
4. M. Santarsiero, F. Gori, R. Borghi, and G. Guattari, "Evaluation of the modal structure of light beams composed of incoherent mixtures of Hermite-Gaussian modes," Appl. Opt. **38**(25), 5272–5281 (1999).
5. X. Xue, H. Wei, and A. G. Kirk, "Intensity-based modal decomposition of optical beams in terms of Hermite-Gaussian functions," J. Opt. Soc. Am. A **17**(6), 1086–1091 (2000).
6. D. Flamm, O. A. Schmidt, C. Schulze, J. Borchardt, T. Kaiser, S. Schröter, and M. Duparré, "Measuring the spatial polarization distribution of multimode beams emerging from passive step-index large-mode-area fibers," Opt. Lett. **35**(20), 3429–3431 (2010).
7. T. Kaiser, D. Flamm, S. Schröter, and M. Duparré, "Complete modal decomposition for optical fibers using CGH-based correlation filters," Opt. Express **17**(11), 9347–9356 (2009).
8. J. W. Nicholson, A. D. Yablon, S. Ramachandran, and S. Ghalmi, "Spatially and spectrally resolved imaging of modal content in large-mode-area fibers," Opt. Express **16**(10), 7233–7243 (2008).
9. D. B. S. Soh, J. Nilsson, S. Baek, C. Codemard, Y. Jeong, and V. Philippov, "Modal power decomposition of beam intensity profiles into linearly polarized modes of multimode optical fibers," J. Opt. Soc. Am. A **21**(7), 1241–1250 (2004).
10. M. Paurisse, L. Lévèque, M. Hanna, F. Druon, and P. Georges, "Complete measurement of fiber modal content by wavefront analysis," Opt. Express **20**(4), 4074–4084 (2012).
11. O. A. Schmidt, C. Schulze, D. Flamm, R. Brüning, T. Kaiser, S. Schröter, and M. Duparré, "Real-time determination of laser beam quality by modal decomposition," Opt. Express **19**(7), 6741–6748 (2011).
12. I. A. Litvin, A. Dudley, and A. Forbes, "Poynting vector and orbital angular momentum density of superpositions of Bessel beams," Opt. Express **19**(18), 16760–16771 (2011).
13. A. Dudley, I. A. Litvin, and A. Forbes, "Quantitative measurement of the orbital angular momentum density of light," Appl. Opt. **51**(7), 823–833 (2012).
14. R. Vasilyeu, A. Dudley, N. Khilo, and A. Forbes, "Generating superpositions of higher-order Bessel beams," Opt. Express **17**(26), 23389–23395 (2009).
15. R. Rop, A. Dudley, C. Lopez-Mariscal, and A. Forbes, "Measuring the rotation rates of superpositions of higher-order Bessel beams," J. Mod. Opt. **59**(3), 259–267 (2012).
16. R. Rop, I. A. Litvin, and A. Forbes, "Generation and propagation dynamics of obstructed and unobstructed rotating orbital angular momentum-carrying Helicon beams," J. Opt. **14**(3), 035702 (2012).
17. A. M. Yao and M. J. Padgett, "Orbital angular momentum: origins, behaviour and applications," Adv. Opt. Photon. **3**(2), 161–204 (2011).
18. G. Li and X. Liu, "Focus Issue: Space multiplexed optical transmission," Opt. Express **19**(17), 16574–16575 (2011).

#164079 - $15.00 USD Received 5 Mar 2012; revised 23 Apr 2012; accepted 24 Apr 2012; published 26 Apr 2012
(C) 2012 OSA

1. Introduction

Techniques to decompose light by use of Fourier optics have been known for a long time, and have been extensively reviewed to date [1]. Historically, these techniques have been applied to pattern recognition problems, and subsequently to the problem of studying the structure and propagation characteristics of laser beams [2–5]. Despite the appropriateness of the techniques, the experiments were nevertheless rather complex. Recently this subject has been revisited by employing computer generated holograms in a mode multiplexing scheme for the modal decomposition of laser beams from fibres [6–10], and for the real-time measurement of the beam quality factor of a laser beam [11]. While these techniques have significant merit, they require a prefabricated diffractive optical element. This implies that information on the modal basis to be used, and the scale parameters of this basis, are known. To date this has been achieved by first modelling the source under study.

In this paper we consider the problem of the azimuthal decomposition of an arbitrary laser source, without any knowledge of the mode structure, the mode phases, or the scale of the amplitude distribution. We make use of a basis comprising the angular harmonics, which are independent of spatial scale, and express the spatial distribution in terms of spatially dependent coefficients in this basis. The result, as we will show, is that the complete decomposition can be achieved without any scale information. We use this to infer directly from measurements of the intensity of the superposition field, its phase, and its orbital angular momentum (OAM) density distribution. In fact, it is clear that since the entire field is known, all physical quantities associated with the field can be inferred. We illustrate the concept by executing a full azimuthal decomposition of: (i) a superposition of two OAM carrying Bessel beams, with relative phase differences and (ii) an off-axis vortex mode. A comparison of our experimental measurements to the predicted theory shows excellent agreement.

2. Concept and theory

The core idea is to expand our unknown field, $u(r,\phi)$, into a basis that is not dependent on scale. Such a basis is the angular harmonics, $\exp(il\varphi)$, that are orthogonal over the azimuthal plane. To illustrate that the azimuthal decomposition that we employ in this work is completely general, we consider, for example, the Laguerre-Gaussian (LG) basis as our OAM basis. An expansion of an arbitrary optical field in terms of this LG basis is given by

$$u(r,\phi) = \sum_{p,l} c'_{p,l} R_{p,l}(r) \exp(il\phi), \tag{1}$$

where $c'_{p,l}$ denotes the complex coefficients and $R_{p,l}(r)$ is the radial part of the LG mode, which only depends on r. One can now combine, and sum over the part of the expression that contains a p-index

$$u(r,\phi) = \sum_{l} \left[\sum_{p} c'_{p,l} R_{p,l}(r) \right] \exp(il\phi) = \sum_{l} c_l(r) \exp(il\phi), \tag{2}$$

where

$$c_l(r) = \sum_{p} c_{p,l} R_{p,l}(r) = a_l(r) \exp\left[i\Delta\theta_l(r)\right]. \tag{3}$$

If the original expansion in terms of the LG modes is completely general, then by implication, so is the azimuthal expansion with the r-dependent coefficients. The coefficients are given by

$$c_l(r) = \frac{1}{2\pi} \int_0^{2\pi} u(r,\phi) \exp(-il\phi) d\phi. \tag{4}$$

#164079 - $15.00 USD Received 5 Mar 2012; revised 23 Apr 2012; accepted 24 Apr 2012; published 26 Apr 2012
(C) 2012 OSA

The coefficient of the azimuthal modes contains information on the spatial distribution of the field. Each coefficient contains an arbitrary phase, $\Delta\theta_l$, relative to some reference, which we may take to be an external source or for convenience the first mode in the series, $l = 0$ at a specific value of r. To describe $u(r,\phi)$ completely, we are required to determine the phase shift between modes and the magnitude of the coefficients. The coefficients may be found by an inner product calculation and a suitable match filter, as shown in Eq. (4). To implement this calculation in a physically realizable manner, consider the signal at the origin of the Fourier plane after a lens (for wavenumber k and focal length f) after the field has been modulated by a transmission function given by $t_l(r,\phi)$

$$U_l(0) = \frac{\exp(i2kf)}{i\lambda f}\int_0^{\infty}\int_0^{2\pi} t_l(r,\phi)u(r,\phi)rdrd\phi. \tag{5}$$

Since we wish to implement Eq. (4), it is clear that the transmission function has two requirements: (i) it should have an azimuthal phase variation opposite to the mode being analyzed, (ii) to select the information as a function of r it should consist of an annular slit centered at $r = R$ and of negligible thickness, ΔR. These conditions are satisfied if the transmission function is defined as

$$t_l(r,\phi) = \begin{cases} \exp(-il\phi) & R-\Delta R/2 < r < R+\Delta R/2 \\ 0 & otherwise \end{cases}. \tag{6}$$

The subscript l in t_l and U_l refer to selecting the l^{th} mode in the expansion of Eq. (2). So that

$$\begin{aligned} \tilde{U}_l(R,0) &= \frac{\exp(i2kf)}{i\lambda f}\int_0^{\infty}\int_0^{2\pi} t_l(r,\phi)u(r,\phi)rdrd\phi \\ &\approx \frac{k\exp(i2kf)}{if}c_l(R)R\Delta R. \end{aligned} \tag{7}$$

By re-arranging the final result in Eq. (7), we find that

$$c_l(R) = \frac{if}{R\Delta Rk\exp(i2kf)}\tilde{U}_l(R,0). \tag{8}$$

Firstly, we note that a measurement of the intensity of the signal, $I_l(R,0)$, at the origin in the Fourier plane returns exactly our desired magnitude of the coefficients, since

$$a_l(R) = \left|c_l(R)\right| = \frac{f}{R\Delta Rk}\sqrt{I_l(R,0)}. \tag{9}$$

Secondly, we note that if we interfere our selected l mode with a reference wave and consider the inner product signal, then the unknown phase of the coefficient, $\Delta\theta_l$, can be found. If $|g|\exp(i\alpha)$ represents the complex amplitude of the reference wave of the origin then the intensity, at the origin, as a function of the phase delay is given by

$$\begin{aligned} \tilde{I}_l(\Delta\theta_l) &= \left|c_l(R)+g\right|^2 \\ &= a_l^2(R)+\left|g\right|^2+2a_l(R)\left|g\right|\cos[\Delta\theta_l(R)-\alpha]. \end{aligned} \tag{10}$$

It is a simple task to invert Eq. (10) to find the unknown phase delay between the modes. With the complete azimuthal decomposition of the field achieved, as in Eq. (2), it is possible to calculate the intensity of the field, $|u(r,\phi)|^2$, the phase of the field, $\arg[u(r,\phi)]$, the Poynting vector [12],

#164079 - $15.00 USD Received 5 Mar 2012; revised 23 Apr 2012; accepted 24 Apr 2012; published 26 Apr 2012
(C) 2012 OSA

$$\mathbf{S} = \frac{\varepsilon_0 \omega c^2}{4}\left[i\left(u\nabla u^* - u^*\nabla u\right) + 2k\left|u\right|^2 \hat{z} \right], \tag{11}$$

and finally the OAM density [13]:

$$L_z = \frac{1}{c^2}\left[\mathbf{r}\times\mathbf{S}\right]_z . \tag{12}$$

The pertinent point here is that at no stage has any assumption been made on the scale of the basis functions. This is because we have elected to scan the field with an annular slit, thereby storing the scale information in the coefficient of a scale invariant basis. The scale of any OAM basis function is set by the radial coordinate. Since the radial coordinate becomes a part of the coefficient functions, the scale parameter is removed from the basis functions, resulting in the remaining azimuthal component becoming independent of scale. We will now show how to implement the technique with a phase-only spatial light modulator (SLM), thus allowing a full azimuthal decomposition of the field with digital holograms.

3. Experimental methodology

The experimental realization of the technique comprises two parts: the generation and then decomposition of the field, and is shown schematically in Fig. 1(a). The first SLM (denoted as SLM_1) was programmed to produce various fields. The two cases that we considered were (i) a superposition of two OAM carrying Bessel beams [14] and (ii) an off-axis vortex mode. A Gaussian beam from a HeNe laser [Fig. 1(b)] was expanded through a 5 × telescope and directed onto the liquid crystal display of SLM_1 (HoloEye, PLUTO-VIS, with 1920 × 1080 pixels of pitch 8 μm and calibrated for a 2π phase shift at λ~633 nm) where the hologram used to generate the field of interest was programmed. For the case where a superposition of two OAM carrying Bessel beams were studied, two annular rings modulated in their azimuthal phase [see Fig. 1(c)] were encoded onto SLM_1. The amplitude transmission of 0 everywhere outside the annular ring and 1 inside the ring was programmed using complex amplitude modulation for amplitude only effects on a phase-only device. The hologram takes the form of a high frequency grating that oscillates between phase values of 0 and π, and it has been shown that this results in the required amplitude transmission of Eq. (6) [15]. We shall refer to this as the checkerboard pattern: see zoomed in section of Fig. 1(c). The result is non-diffracting petal-like modes [Fig. 1(d)] that rotate as they propagate, and have been studied in detail elsewhere [15,16].

These fields were then magnified with a 10 × objective and directed to the second SLM (SLM_2) for executing the azimuthal decomposition. This was accomplished by executing an inner product of the incoming field with the match filter set to $\exp(il\phi)$, for various l values, and for particular radial (r) positions on the field, as given by Eq. (6) and illustrated in Fig. 1(e). The typical width of the ring in the experiments was ΔR = 80 μm. The width of the ring, as well as the azimuthal index (l) encoded within the ring, are limited by the resolution of the SLM. The field at the Fourier plane is shown in Fig. 1(f) – note that we only require the intensity at the origin of this plane.

#164079 - $15.00 USD Received 5 Mar 2012; revised 23 Apr 2012; accepted 24 Apr 2012; published 26 Apr 2012
(C) 2012 OSA

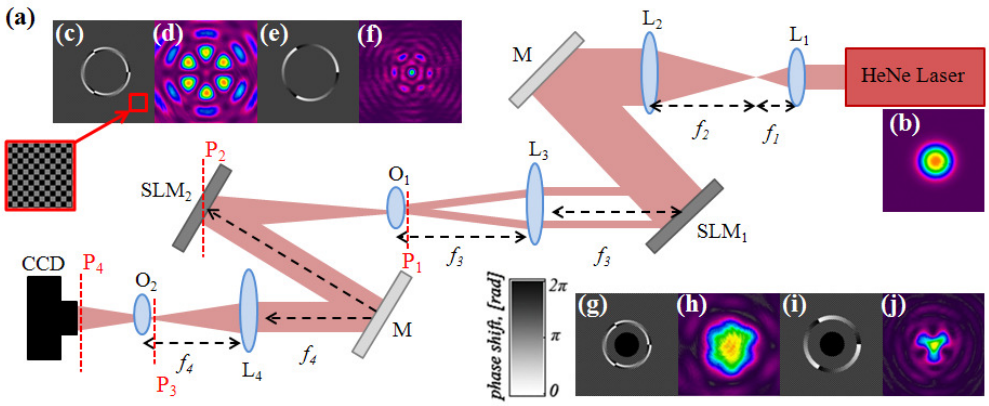

Fig. 1. (a) A schematic of the experimental setup for performing the modal decomposition. L: Lens (f_1 = 15 mm; f_2 = 75 mm; f_3 = 200 mm and f_4 = 200 mm); M: Mirror; SLM: Spatial Light Modulator; O: Objective; CCD: CCD Camera. The objective, O_2, was placed at the focus (or Fourier plane) of lens, L_4. Lens L_3 and L_4 perform a Fourier transform of SLM_1 and SLM_2, respectively, in a 2-*f* system. Objectives O_1 and O_2 are telescopes which image and magnify both the phase and amplitude of the fields at planes P_1 and P_3 to planes P_2 and P_4, respectively. (b) The Gaussian beam used to illuminate SLM_1. (c) The digital hologram used to generate the optical field of interest (d) and the digital hologram (e) used to extract the weightings of the modes from the inner product (f). The digital holograms for generating (g) and decomposing (i) the field, to extract the intermodal phase. The intensity profile of the field at the plane of SLM_2 (h) and CCD (j). Each hologram has a checkerboard pattern, shown as an inset to (c).

In order to measure the phase delay between the modes, we switch off the checkerboard pattern in the centre of both SLMs. This results in a portion of the initial Gaussian beam passing through the entire optical system, without "seeing" the phase holograms. Because it follows the same path as the modes that we wish to study, we can use the central peak of the beam as our reference beam, $|g|\exp(i\alpha)$. Figure 1(g) shows the initial generating step but with a constant phase in the centre of the hologram (black disk), the resulting mixing with the non-diffracting petals [Fig. 1(h)] and after passing through the second SLM [Fig. 1(i)] the resulting interference of the waves [Fig. 1(j)]. The constant phase of the reference could be changed across several values to provide information on the quadrant of the cosine function in Eq. (10). Note that switching between the intensity measurement [Figs. 1(c)–1(f)] and the phase measurement [Figs. 1(g)–1(j)], we require only a change in the holograms loaded onto SLMs 1 and 2. This switching between holograms can be done at 60 Hz, i.e., practically real-time acquisition of the necessary data.

4. Results and discussion

4.1. Superposition of two OAM carrying Bessel beams

To test the accuracy of the method, we first created a superposition of two Bessel beams with opposite handedness, i.e., $m = 3$ and $n = -3$ and defined generally as

$$u(r,\phi) = A_m J_m(kr)\exp(im\phi) + A_n J_n(kr)\exp(in\phi)\exp(i\Delta\theta). \qquad (13)$$

The phase delay, $\Delta\theta$, in Eq. (13) was then varied between 0 and 2π, resulting in a rotation of the intensity pattern, which can easily be measured by observing the angular displacement of any one of the petals. This measured rotation is directly related to $\Delta\theta$, thus allowing the measured phase shift to be compared to the programmed value. The programmed phase shift and resulting petal rotation are shown in Fig. 2(a), and compared to the theoretical rotation. The results of this calibration test are shown in Fig. 2(b), where it is clear that the agreement between measured and actual is very good (slope difference of 0.1%). The error bars were determined through a range of intensity values in the finite region (few pixels) around the

#164079 - $15.00 USD Received 5 Mar 2012; revised 23 Apr 2012; accepted 24 Apr 2012; published 26 Apr 2012
(C) 2012 OSA

origin of the Fourier plane. These results confirm that the setup was working correctly without spurious effects.

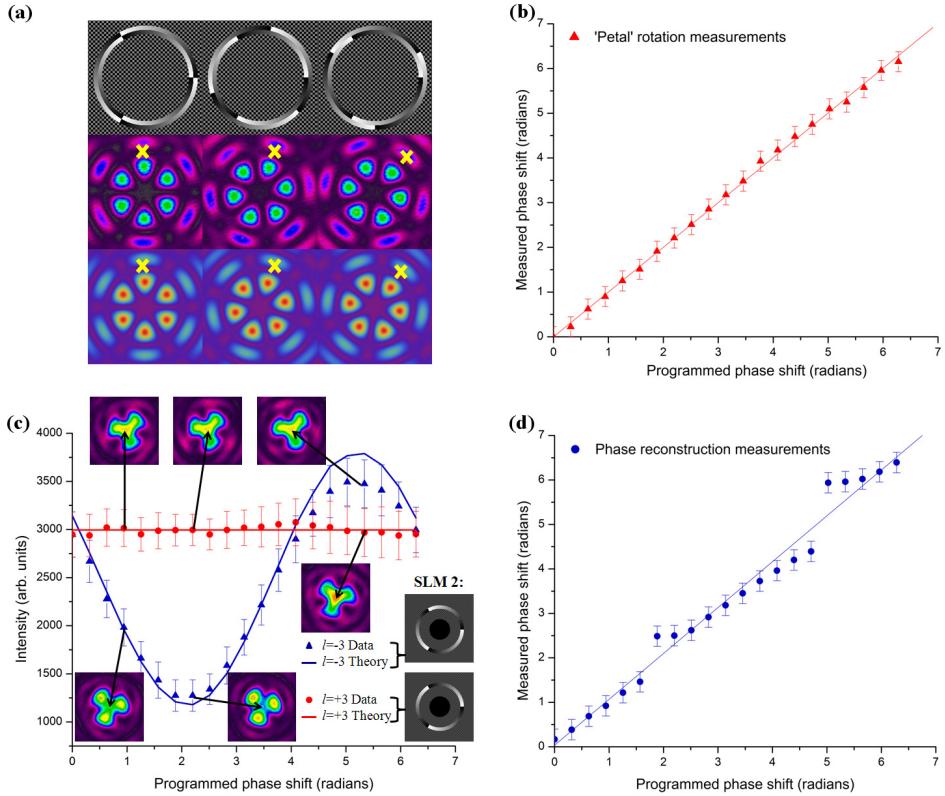

Fig. 2. (a) If the phase is shifted in one of the modes in the initial field (top row), then the measured petal structure of the superposition field (middle row) is seen to rotate, as predicted by theory (bottom row); (b) comparison of the measured phase shift to the actual phase shift; (c) interference of the modes with a reference wave results in changing intensity at the origin of the Fourier plane, which can be used to infer the phase shift per mode; (d) comparison of the measured phase shift to the actual phase shift (see Media 1 and Media 2).

Next, the programmed phase shift $\Delta\theta$ was measured using the interference technique and analyzed using Eq. (10). The phase shift in the $n = -3$ beam was scanned through 0 to 2π and the interference monitored, as shown in Fig. 2(c). By removing the offset phase of the reference beam (corresponding to the maximum in the interference signal), the measured phase could be compared to the programmed phase. The results are also shown in Fig. 2(d), and again the agreement is good (slope difference of 3%), but with some uncertainty near a programmed phase shift of 0.60π and 1.60π; these discontinuities occur at maxima and minima in the interference intensity [Fig. 2(c)], and are due to the flatness of the change in the measured intensity for a change in phase value (three values were used to uniquely determine the phase). To illustrate further that the technique works, we constructed a superposition field with $m = +3$ and $n = -2$, to deliberately break the symmetry of the field. The annular ring on SLM_2, of width 80 μm, was scanned through 28 radial positions (maximum number to scan our field) and the azimuthal phase varied across $l \in [-10,10]$. The only non-zero components (>0.5% of the modal power) were those corresponding to $l = +3$ and $l = -2$, which contained ~95% of the modal power. With all the unknown terms in Eq. (4) measured experimentally, we were able to reconstruct the intensity and phase of the initial field, and compare it to the theoretical prediction (based on our own hologram function on SLM_1). The results for the intensity of the field are shown in Figs. 3(a) and 3(d) while that

#164079 - $15.00 USD Received 5 Mar 2012; revised 23 Apr 2012; accepted 24 Apr 2012; published 26 Apr 2012
(C) 2012 OSA

of the phase of the field is given in Figs. 3(b) and 3(e). There is very good agreement between the theoretically predicted field and the field reconstructed from the azimuthal decomposition.

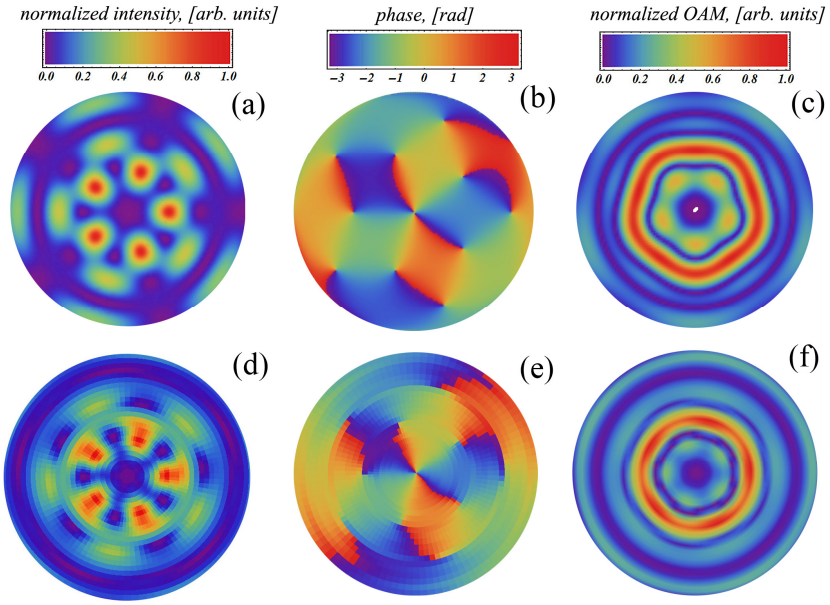

Fig. 3. A comparison of the theoretical (top row) and the experimentally reconstructed (bottom row) images of the (a, d) intensity, (b, e) phase, and (c, f) OAM density of the light.

An interesting application of this technique is the determination of the complete OAM density of the field. It has been known for some time now that photons carry orbital angular momentum ([17] and references therein), yet it remains a challenge to measure the local and global OAM of a field in a manner that is quantitative. Previously we have attempted such measurements without the phase information, and found success for particular structures of optical fields [12,13]. With a full azimuthal decomposition of the field, including the phase delays, we can infer the OAM density of *any* field directly from our measurement. The theoretical and experimental results of this are shown in Figs. 3(c) and 3(f), respectively, and are in agreement.

4.2. Off-axis vortex mode

Next we apply our decomposition technique to the example of a Gaussian beam with an off-axis vortex. The results are presented in Fig. 4.

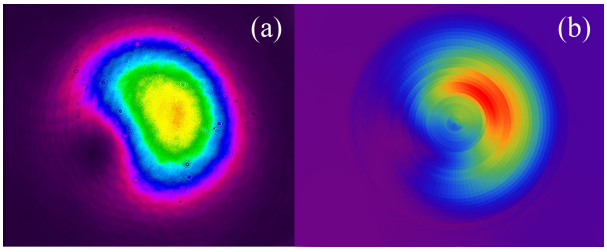

Fig. 4. A comparison of the experimentally recorded intensity (a) and the reconstructed intensity (b), for the off-axis vortex case, created from a superposition of Hermite-Gaussian modes.

#164079 - $15.00 USD Received 5 Mar 2012; revised 23 Apr 2012; accepted 24 Apr 2012; published 26 Apr 2012
(C) 2012 OSA

The same measurement procedure, as that discussed above, was implemented on the field, whose experimentally recorded intensity profile is given in Fig. 4(a). The reconstructed field is shown in Fig. 4(b) illustrating that this technique is successful in the reconstruction of optical fields which possess an on-axis intensity. The problem in this case is that there is no dark core in the centre of the field under investigation where we could pass a Gaussian reference beam through, for the implementation of the phase measurements. In this case we use a section of the field under investigation as our reference (assuming no singularities, a single pixel size region will have a uniform phase).

4.3. Alignment sensitivity

Although one can represent the beam in terms of expansions with respect to any beam-axis, the coefficients in the expansions are sensitive to a shift of the beam-axis. Here, our concern is the fidelity of the reproduced beam rather than the fidelity of the expansion coefficients. Naturally we do not want the beam-axis to be too far off, because that would increase the higher-order coefficients and reduce the fidelity of the reconstructed beam, but small shifts in the beam axis does not pose a serious problem and this is illustrated in Fig. 5(a). The hologram on SLM_2 was displaced with respects to the propagation axis of the field under investigation for step sizes of a single pixel (i.e. 8 μm) and the fluctuation in the on-axis intensity of the inner product, from which the unknown field is reconstructed, shows very little variation (the percentage error is roughly 0.5% per pixel shift). It is fairly easy to get the alignment of our system within such distances from the actual beam axis. If the displacement is much greater (10 times greater) then the alignment does pose a problem and the on-axis intensity of the inner product varies significantly, evident in Fig. 5(b).

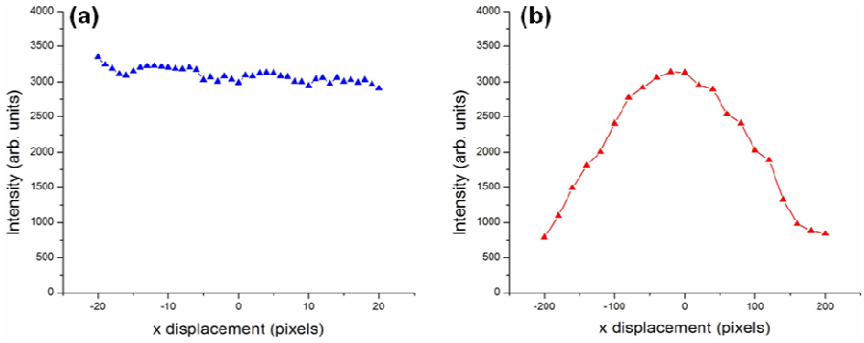

Fig. 5. Graph of the measured on-axis intensity of the inner product as a function of a lateral displacement of the hologram on SLM_2 for a displacement range of (a) –20 to 20 pixels (–160 μm to 160 μm) and (b) –200 to 200 pixels (–1600 μm to 1600 μm).

For the experimental measurements presented here we aligned each SLM to a common propagation axis by initially centering each SLM on a Gaussian mode that propagated through the system. More general alignment techniques, as used by other decomposition methods, could also be employed [6,7].

5. Conclusion

We have outlined an improved method for the azimuthal decomposition of an arbitrary field that requires no scale information of the basis functions, and allows for the phases to be easily measured. It is significant to note that using only minor changes to the digital holograms, we can switch the setup between measuring azimuthal weights to azimuthal phase delays – no optical re-alignment is necessary, and no path length adjustment is required for the phase measurements. Moreover, even though our system is not automated and a scan of all measurements would take 4 hours, in an automated system the holograms can be displayed at fast refresh rates (60 Hz), so that the measurement per radial position takes about 1 s. Using superpositions of OAM carrying Bessel beams as an example, we have

#164079 - $15.00 USD Received 5 Mar 2012; revised 23 Apr 2012; accepted 24 Apr 2012; published 26 Apr 2012
(C) 2012 OSA

shown excellent reconstruction of both the intensity and phase of the field, as well as the OAM density everywhere in the field. We have also shown accurate reconstruction of an off-axis vortex beam, illustrating the versatility of the method. This technique will surely be of relevance to those working in OAM, both at the classical and quantum level, as well as to the emerging field of mode multiplexing for future telecommunications ([18], and references therein), where mode generation and decomposition are necessary tools.

#164079 - $15.00 USD Received 5 Mar 2012; revised 23 Apr 2012; accepted 24 Apr 2012; published 26 Apr 2012
(C) 2012 OSA